

# The protein concentration gradient within eye lens might originate from constant osmotic pressure coupled to differential interactive properties of crystallins

F. V  r  tout and A. Tardieu

Centre de G  n  tique Mol  culaire, CNRS, F-91190 Gif sur Yvette, France

Received December 20, 1988/Accepted in revised form March 17, 1989

**Abstract.** A protein concentration gradient exists from the center to the periphery of most lenses, the origin of which is still a matter of debate. The gradient, which contributes to the lens optical quality, seems to be accompanied by an uneven distribution of the crystallin classes, with the nucleus usually enriched in  $\gamma$ - and the cortex in  $\alpha$ -crystallins. Since the osmotic pressure within the lens seems to be constant and since a rather different interaction behaviour of  $\alpha$ - and  $\gamma$ -crystallins was demonstrated in previous studies, we propose that the maintenance of a constant osmotic pressure through the lens is sufficient to induce and stabilize a protein concentration gradient. The theoretical treatment has been worked out and the validity of the hypothesis has been demonstrated with colloidal osmotic pressure measurements of lens cortical and nuclear cytoplasmic extracts as a function of protein concentration. To account for the *observed* lens concentration gradient, however, a small additional concentration gradient in the opposite direction, involving an ion or small molecule, might be required.

**Key words:** Eye lens, osmotic pressure, crystallins, concentration gradient

## Introduction

The biological function of the eye lens is linked to macroscopic physical properties themselves determined by local structure and composition. Mammalian lenses are made of regularly stacked fiber cells which enclose, as a major component, high concentrations of lens specific proteins, the crystallins. The high crystallin concentrations provide the refractive index required for the lens to play its role, while crystallin structure and overall repulsive interactions account for lens transparency (Trok  l 1962; Benedek 1971; De-

laye and Tardieu 1983; Tardieu and Delaye 1988; V  r  tout et al. 1989).

Aside from such properties, the presence of a protein concentration gradient in mammalian lenses has been demonstrated by a variety of techniques, e.g. refractive index measurements (Campbell 1984), biochemical analysis (Siezen et al. 1988) and Raman spectroscopy (Huizinga et al. 1988). The precise shape of this gradient may vary from species to species. Measured along the optic axis, the refractive index gradient resembles a parabola in rat (Campbell 1984) or rabbit (Huizinga et al. 1988) while it presents a more complicated shape in human lens (Huizinga et al. 1988). The gradient is generally thought to play a role in reducing optical aberrations of the visual system. The absolute protein concentration values derived from measurements of the gradient may be subject to some uncertainties, since other data such as crystallin extinction coefficients or refractive index increments are required (Pierscionek et al. 1987). Such uncertainties, however, do not question the general existence of a steep concentration gradient from cortex to nucleus (although the gradient is not very steep in man). In calf and rabbit lenses the protein concentration was reported to vary from about 20% to 45%–50% from cortex to nucleus (Huizinga et al. 1988; Amoore et al. 1959) while higher values, from about 55% to 70%, were calculated from measurements on the rat nucleus (Campbell 1984; Siezen et al. 1988). The situation in birds, reptiles and fish is less well documented and will not be considered here.

The origin of the protein concentration gradient has been the subject of speculation. From the molecular standpoint, the reason for the gradient must be sought in the individual properties of the various crystallins. Three crystallin classes are distinguished,  $\alpha$ ,  $\beta$  and  $\gamma$ , which correspond to three different gene families and differ in addition by molecular weight, charge, and interactive properties (Slingsby 1985). It is now well documented, in particular in mammals, that the

foetal lens becomes the adult lens nucleus during morphogenesis, while differential gene expression occurs during embryogenesis and development (Piatigorsky 1981). As a result, the lens nucleus is enriched in low molecular weight  $\gamma$ - while the lens cortex is enriched in  $\alpha$ -crystallins (Siezen et al. 1988). How different crystallin properties could be translated into a protein concentration gradient remains, however, unclear.

Macroscopic measurements of ion, water and small solute fluxes show that the lens volume, as well as the water and small metabolite content, is mainly determined by osmotic equilibration with the surrounding medium, i.e. the circulating aqueous humor and the vitreous humor. A lens acts as an almost perfect osmometer in quite a large range of applied osmotic pressures and changes its water volume and intracellular solute concentrations accordingly (Cotlier et al. 1968). The presence of proteins seems hardly relevant to such processes. How the lens maintains and regulates its osmotic pressure equilibrium with the exterior is not completely understood. It is, however, well known that the cation distribution within a lens is actively controlled by a Na/K ATPase located in the anterior epithelial cell layer while passive Na transport occurs on the posterior side. In addition, for such properties the compartmentation of the lens into fiber cells does not need to be taken into account since the lens behaves essentially as if it were a single, macroscopic cell. For instance, the intracellular cation distribution, i.e. the cation distribution within the lens ( $\text{Na}^+$  about 25 mM and  $\text{K}^+$  150 mM as compared to extracellular  $\text{Na}^+$  130 mM and  $\text{K}^+$  6 mM, Duncan and Jacob, 1984) has been modelled by a single cell pump-leak mechanism (Kinsey and Reddy 1965). The situation probably originates from almost free circulation of water, ions and low molecular weight metabolites within the normal lens through the many gap junctions found between fiber cells (Goodenough et al. 1980).

We argue in this paper that it is possible to gather these separate pieces together and make sense of the whole. In a recent study (Vérétout et al. 1989), the *colloidal* osmotic pressure of  $\alpha$ -crystallins was measured as a function of protein concentration in buffers of different ionic strength. This *colloidal* osmotic pressure was shown to be strongly dependent, especially at high protein concentration, upon protein quaternary structure and protein-protein interactions. In addition,  $\alpha$ -crystallins display repulsive and  $\gamma$ -crystallins display attractive interactions. As a consequence, the *colloidal* osmotic pressure of two solutions made of the same number but different types of crystallins may be different and conversely, solutions made with two different types of crystallins and equilibrated at the same *colloidal* osmotic pressure may have different final protein concentrations. It is therefore tempting to

visualize the lens fiber cells as a series of concentric dialysis bags, the protein composition of which varies from the lens nucleus to the cortex, themselves surrounded by a larger dialysis bag, the capsule. The whole system is constantly equilibrated against aqueous and vitreous humor, so that the external and the internal osmotic pressure are the same. Such an equilibration should lead to variation, from the lens nucleus to the cortex, of the final protein concentration.

All of these considerations lead us to formulate the following hypothesis: *constant applied osmotic pressure, coupled to differential interactive properties of crystallins, is sufficient to induce a protein concentration gradient within the eye lens.*

In the present article, we first develop the theoretical basis of such an hypothesis. We then present experiments designed to test the hypothesis: the measurement of the *colloidal* osmotic pressure of nuclear and cortical cytoplasmic extracts from calf lenses as a function of protein concentration. The results obtained are then compared to the observed concentration gradient and finally, some expected consequences of the hypothesis are discussed.

### Theoretical presentation of the problem

For 'ideal' solutions, the variation of the osmotic pressure  $\Pi$  (dynes/cm<sup>2</sup>) is linear with the number,  $n$ , of solute particles per unit volume (cm<sup>3</sup>) of solution:

$$\Pi = (n/N_a) R T, \quad (1)$$

where  $R$  ( $8.31 \cdot 10^7$ ) is the gas constant,  $T$  (°K) the absolute temperature and  $N_a$  Avogadro's number. With a monodisperse solution, the osmotic pressure may be simply expressed as a function of the molarity  $M$  (moles/litre) of the solute particles:

$$\Pi = 10^{-3} M R T. \quad (2)$$

The osmotic pressure of a buffered solution of macromolecules is conveniently divided into two parts. The first one is the osmotic pressure  $\Pi_s = \sum \Pi_{si}$ , i.e. the sum due to the ions and small solute particles (amino-acids, sugars...) that are free to circulate across a dialysis membrane. The second one is the osmotic pressure  $\Pi_{col}$  for the macromolecular solute to which the membranes are impermeant – which is usually referred to as the *colloidal* osmotic pressure of the solution.

$$\Pi = \sum \Pi_{si} + \Pi_{col} \quad (3)$$

since the number of proteins per unit volume may be simply expressed as a function of the protein concentration  $c$  (g/cm<sup>3</sup>) and, for a polydisperse system, of the

number average molecular weight  $M_n$ , the colloidal osmotic pressure is often written (Eisenberg 1976):

$$\Pi_{\text{col}} = c R T / M_n, \quad (4)$$

where

$$M_n = \sum c_i / \sum (c_i / M_i). \quad (5)$$

With a real solution, the situation may be much more complicated since any type of solute–solute and/or solute–solvent interaction is likely to modify the osmotic pressure, as Reiff (1986) has pointed out. The reason why analysis of the solution properties remains possible is that in a number of cases a few of these effects are predominant so that the others can be neglected.

From previous work on lens proteins, it appeared that at physiological pH and ionic strength, departure from ideality can be treated independently for the protein and for the ions (and small solutes). For the latter, departure from ideality is conveniently accounted for by introducing activity coefficients. The problem is to express departure from ideality of the protein solutions. This can be done in different ways. In the thermodynamic approach, the colloidal osmotic pressure is often expanded as a series of virial coefficients (Eisenberg 1976). A structural approach can also be used. The normalized X-ray scattering of a monodisperse protein solution as a function of the scattering angle  $s = 2 \sin \theta / \lambda$  may be written as:

$$I(c, s) = I(0, s) S(c, s), \quad (6)$$

where  $I(0, s)$  is the intensity that would be scattered in the ‘ideal’ case and where  $S(c, s)$ , called the structure factor of the solution, corresponds to the Fourier transform of the spherically averaged auto-correlation function of the particle distribution. Since the particle distribution is itself determined by the interactions, the shape of  $S(c, s)$  is characteristic of the interactions. The relationship with colloidal osmotic pressure is (Guinier and Fournet 1955; V  r  tout et al. 1989):

$$\Pi_{\text{col}} = c R T / M_n \int_0^c (dc / S(c, 0)). \quad (7)$$

In the case of polydisperse mixtures Eq. (7) is no longer strictly valid, yet still represents a good and simple approximation of the thermodynamic–structure relationship.

Figure 1 summarizes some results previously obtained on lens  $\alpha$ - and  $\gamma$ -crystallins. The variation of the colloidal osmotic pressure with molecular weight and interactive properties is illustrated schematically. The measured colloidal osmotic pressure of  $\alpha$ -crystallins increases, with protein concentration, much more rapidly than expected for the ideal case as calculated from Eq. (4) (positive virial coefficient). Using a combination of osmotic pressure and X-ray scattering exper-

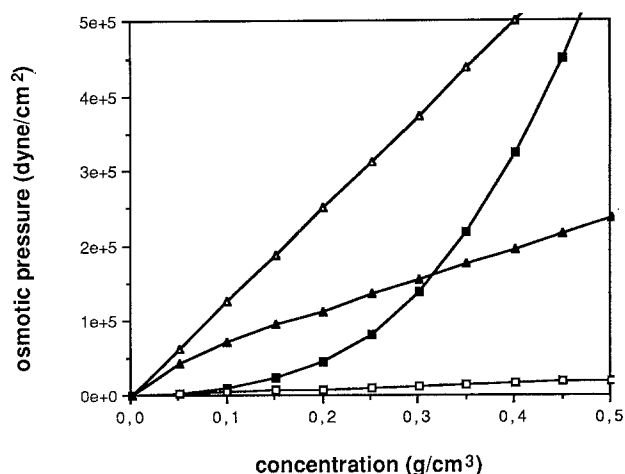


**Fig. 1.** *Open symbols:* osmotic pressure calculated in the ‘ideal case’ for particles with molecular weights equal respectively to those of  $\alpha$ - (square) and  $\gamma$ -crystallins (triangles). *Full symbols:* osmotic pressure measured with  $\alpha$ - (square) and  $\gamma$ -crystallins (triangles). ( $\Pi$  is often expressed in the literature in mOsmoles. From Eq. (2), it can be calculated that the osmotic pressure of 1 mM of particles at room temperature is about  $2.5 \cdot 10^4$  dynes/cm<sup>2</sup>)

iments, such behaviour was shown to be determined by solute–solute electrostatic screened coulombic interactions. The interaction could be modelled by a small number of parameters: charge, excluded volume and diameter of the solute particles (V  r  tout et al. 1989). According to the overall shape of the X-ray scattering curves, the predominant overall interaction in cortical cytoplasmic extracts (Delaye and Tardieu 1983) and nuclear cytoplasmic extracts (unpublished observations) from calf lenses is also an electrostatic repulsive solute–solute interaction.

Preliminary X-ray and osmotic pressure experiments on calf lens  $\gamma$ -crystallins demonstrated a different behaviour. The corresponding variation of the colloidal osmotic pressure is also illustrated in Fig. 1. Since the  $\gamma$ -crystallin molecular weight is much lower than the  $\alpha$ -crystallin molecular weight, the osmotic pressure calculated in the ideal case is much higher. The measured colloidal osmotic pressure was also found to increase with protein concentration, yet, much less rapidly than in the ideal case (negative virial coefficient). Such a variation coupled to the X-ray data (unpublished results) may be accounted for by ‘attractive’ solute–solute interactions leading to uneven distribution of the solute particles. This attractive interaction could be linked to the ion-pair distribution on the  $\gamma$ -crystallin surface (Wistow et al. 1983) and probably plays a role in the phase separation that  $\gamma$ -crystallins undergo with decreasing temperature (Siezen et al. 1985; Thomson et al. 1987). The interaction has not yet, however, been satisfactorily modelled with structural parameters.

We have emphasized so far how differences in protein molecular weight and/or interactive properties are reflected in differences in the colloidal osmotic pressure. Figure 1 also shows that it is possible to end up with colloidal osmotic pressure of the same order of magnitude if the low molecular weight proteins interact through attractive interactions and the high molecular weight proteins through repulsive ones.

Applying these theoretical tools to the case of the lens might seem easy. However, attempts to predict from Eq. (7) and the experiments summarized in Fig. 1 whether the colloidal osmotic pressure of lens cortical cytoplasmic extracts may be higher or lower than that of nuclear cytoplasmic extracts at the same protein concentration leads us to the following interesting situation. Since the nucleus is enriched in low molecular weight  $\gamma$ -crystallins,  $M_n$  is likely to be lower for nuclear than for cortical extracts. Since the  $\gamma$ -crystallin interactions appear to be attractive while the  $\alpha$ -crystallin interactions are repulsive,  $S(c, 0)$  is likely to be higher for nuclear than for cortical extracts at a given protein concentration. Therefore, and although the expression of colloidal osmotic pressure in Eq. (7) might seem at first sight rather simple, the result of increasing  $\gamma$ -crystallin with respect to  $\alpha$ -crystallin concentration is hardly predictable since it is expected to both increase osmotic pressure by decreasing  $M_n$  and decrease osmotic pressure by increasing  $S(c, 0)$ . Consequently, we decided to measure the colloidal osmotic pressure, as a function of protein concentration, of both nuclear and cortical cytoplasmic extracts.

## Materials and methods

### *Preparation of the lens cytoplasmic extracts*

Cytoplasmic extracts were prepared from 4-month-old calf lenses. Lenses were dissected and cooled to 4°C to induce the nuclear opacity referred to as cold cataract. Nucleus and cortex, defined here as respectively the opaque and transparent parts of the lens, can thus be simply separated. Nucleus and cortex were separately homogenized in 4 volumes of a physiological phosphate buffer pH 6.8, ionic strength  $I = 150$  mM, adjusted with KCl, supplemented with  $\text{NaN}_3$ , dithiothreitol and phenylmethylsulfonylfluoride (Clark et al. 1982; Delaye et al. 1987). The solution was centrifuged for 30 mn at 10,000 g to separate the membrane fragments and kept as a stock solution at 4°C.

### *Chromatography*

Analysis of the composition of the cytoplasmic extracts was performed with a fractogel (TSK-HW55S)

column ( $vol = 600 \text{ cm}^3$ ,  $h = 100 \text{ cm}$ ) eluted at 4°C and about  $30 \text{ cm}^3/\text{h}$  with the preparation buffer. Possible variation with time of the elution profiles was checked with HPLC. For HPLC, a Beckman apparatus was used with a 30 cm SW4000 TSK column. Samples were diluted with the buffer used for the preparation to reach a final protein concentration between  $c = 0.2 \cdot 10^{-3}$  and  $c = 2 \cdot 10^{-3} \text{ g/cm}^3$ . 50 to 100  $\mu\text{l}$  of this sample was injected and eluted at  $0.5 \text{ cm}^3/\text{mn}$  at 20°C. Elution was detected by UV absorbance. Extinction coefficients at 280 nm  $A_{1\text{cm}}^{1\%}$  were taken to be: 8.45 for  $\alpha$ -, 20 for  $\gamma$ - and 23 for  $\beta$ -crystallins.

### *Osmotic pressure*

The osmotic pressure of the cytoplasmic solutions was measured using a secondary osmometer directly copied from that designed and described by Prouty et al. (1985). Briefly, the solution of interest is equilibrated against dextran T500, the osmotic pressure of which is known (Parsegian et al. 1986; V  r  tout et al. 1989). The following relationships were used, where  $w$  is the weight % of dextran:

$$w < 0.1 \text{ g/g} : \log \Pi = 2.48 + 1.05 w^{0.416} \quad (\text{V  r  tout et al. 1989})$$

$$w > 0.1 \text{ g/g} : \log \Pi = 2.75 + 1.03 w^{0.383} \quad (\text{Parsegian et al. 1986})$$

For most experiments we used a beaker (volume  $250 \text{ cm}^3$ ) in which four bags of protein solution, two of cortical and two of nuclear cytoplasmic extracts, could be equilibrated at the same time. The dialysis bag was Spectrapor 2, 6.4 mm flat width, cutoff 14,000.

The experiments were performed at  $I = 150$  mM pH 6.8, close to the physiological values. In these conditions, the crystallin charge is essentially screened. In addition, the Donnan effect is calculated to remain negligible.

For convenience, the experiments were done at room temperature. They were performed as quickly as possible to minimize changes with time of the crystallin molecular weights. The time needed for equilibration was 6 to 10 days.

Cortical and nuclear extract concentrations were measured either by dry weight, using a Speed Vac concentrator, or by refractive measurements, using an Abbe refractometer. The refractive index calibration curve versus concentration  $c$  ( $\text{g/cm}^3$ ) was itself established using dry weight to yield the following relationship that was found similar to previous determinations (Delaye et al. 1987):

$$n = 1.336 + 0.184 c .$$

## Results

### Composition of nuclear and cortical cytoplasmic extracts

The elution profiles of the nuclear and cortical cytoplasmic extracts loaded on the fractogel column are shown in Fig. 2. These profiles were found to be quite reproducible from one preparation to the next (not shown). The various crystallin classes can be easily identified from the shape of the profiles. Such an identification was, however, checked using isoelectrofocusing agarose and SDS polyacrylamide gel electrophoresis (not shown). From the profiles, the relative proportions of  $\alpha$ -,  $\beta_H$ -,  $\beta_L$  and  $\gamma$ -crystallins were estimated. They are given in Table 1. Figure 2 and Table 1 clearly show that the separation of cortical and nuclear cytoplasmic extracts indeed resulted in rather different crystallin composition in the two types of extracts, as often reported (e.g. Bindels 1982). The nuclear extracts present a small amount of high molecular weight aggregates eluting with the void volume (visible on the HPLC profile), then an  $\alpha$ -peak but the major feature of the profile is the importance of  $\beta_L$  and  $\gamma$ -crystallin peaks. The cortical extract profile presents a major  $\alpha$ -crystallin peak and a higher proportion of  $\beta_H$ -crystallins.

These features are also easily recognizable on the HPLC profiles, where the high molecular weight compounds are particularly well resolved at the expense of the low molecular weight ones (Fig. 2). The profiles were found to be independent of the sample concentration, before dilution for the HPLC experiment. The profiles were only slightly modified after the osmotic pressure measurements (Fig. 2). The relative amount of  $\beta_L$  with respect to  $\beta_H$ -crystallins was decreased in the nuclear extracts while the cortical extracts were essentially unchanged. No change could be detected in the average  $\alpha$ -crystallin molecular weight.

A rough estimation of  $M_n$  was obtained from the profiles of Fig. 2 and Eq. (5), which is also given in Table 1. Although such an estimation cannot be very precise,  $M_n$  seems definitely lower in nuclear than in cortical extracts (note that, because of the form of Eq. (5),  $M_n$  is mainly determined by the low molecular weight compounds). The changes observed after the osmotic stress experiments with nuclear extracts do not result in significant variations of the calculated  $M_n$ .

### Osmotic stress experiments

The *colloidal* osmotic pressure measured as a function of protein concentration for both cortical and nuclear cytoplasmic extracts is shown in Fig. 3a and b, representing two different sets of experiments performed with two different batches of calf lenses. It can be seen

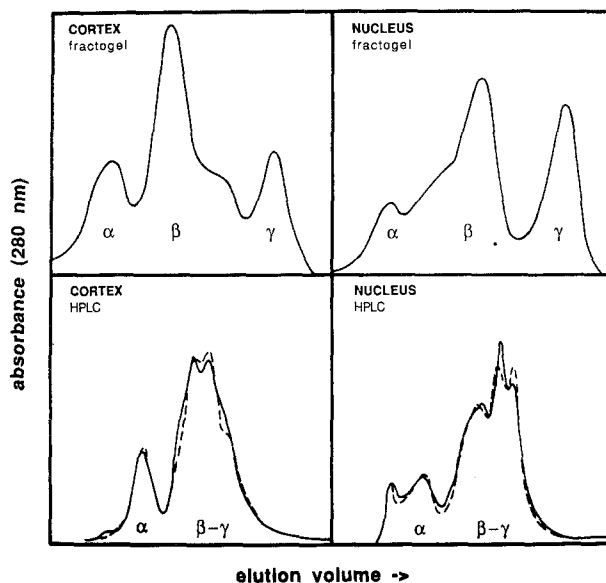


Fig. 2. Elution profiles of cortical and nuclear cytoplasmic extracts. Top: fractogel column; bottom: HPLC: solid line and dashed line, before and after osmotic pressure measurements

Table 1. Protein composition (%) and number average molecular weight

	$\alpha$	$\beta_H$	$\beta_L$	$\gamma$	$M_n$
Cortical extracts	41.1	37.9	7.8	13.2	109,000
Nuclear extracts	20.6	24.7	24.2	30.5	47,000

that the two preparations display essentially the same behavior, the curves are almost superimposable (which means that our separation between cortical and nuclear extracts was quite reproducible). The colloidal osmotic pressure versus concentration relationship has indeed the shape expected for solute-solute repulsive interactions: the colloidal osmotic pressure increases with protein concentration much more rapidly than would be expected in the ideal case. In addition, at high protein concentration, the colloidal osmotic pressure of the cortical cytoplasmic extracts increases more rapidly with protein concentration than that of the nuclear cytoplasmic extracts.

More precisely, the colloidal osmotic pressure of cortical and nuclear cytoplasmic extracts are indistinguishable until  $c = 0.200 \text{ g/cm}^3$ . The precision of the measurement is, however, limited in this region since the equilibrium is slow and difficult to reach (as a consequence,  $M_n$  cannot be determined from the initial slope using Eq. (4)).

For protein concentrations higher than  $c = 0.200 \text{ g/cm}^3$ , the absolute protein concentration is determined within about 2% accuracy. The concentra-

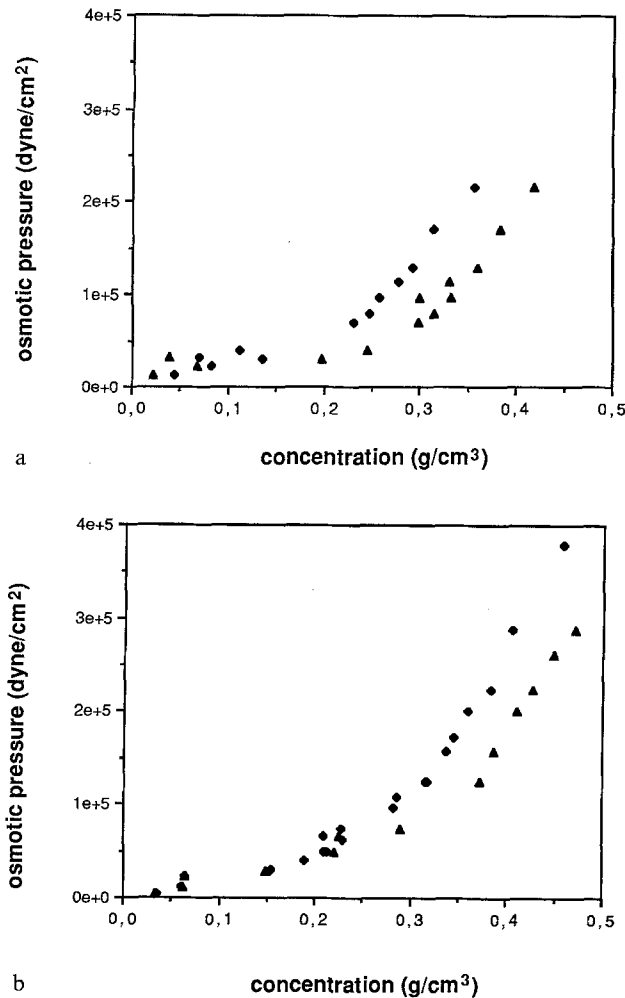


Fig. 3. Colloidal osmotic pressure versus protein concentration measured for (triangles) nuclear and (diamonds) cortical cytoplasmic extracts from calf lenses. a and b correspond to two different batches of calf lenses

tion difference between cortical and nuclear cytoplasmic extracts at a given colloidal osmotic pressure is more accurate, within 1%, since both experiments are performed at the same time in exactly the same conditions. It is thus clear from Fig. 3 that at high protein concentrations, for a given applied *colloidal* osmotic pressure, the concentration of the nuclear extracts is systematically and significantly higher than that of the cortical extracts. For instance, at  $\Pi = 2.2 \cdot 10^5$  dynes/cm<sup>2</sup> the concentration difference is 4.3% in the first and 6% in the second series of experiments.

Figure 3 thus demonstrates the validity of our hypothesis. More precisely, what is shown in Fig. 3 is that a constant applied *colloidal* osmotic pressure coupled to different interactive properties of the crystallins is sufficient to induce an average protein concentration difference in cortical and nuclear extracts of about 5%. Figure 3 also provides us with the order of magnitude of the colloidal osmotic pressure at physiological

protein concentration. Since  $2.5 \cdot 10^4$  dynes/cm<sup>2</sup> correspond to about 1 mOsmole, it appears that when the protein concentration is of the order of  $0.40 \text{ g/cm}^3$ , the colloidal osmotic pressure of the cortical and nuclear extracts is respectively 10 and 7 mOsmoles. Finally, Fig. 3 shows that in the physiological protein concentration range, a change in protein concentration of  $0.020 \text{ g/cm}^3$  is equivalent to a change in ion or small solute osmolarity of 1 mOsmole.

## Discussion

In our experiments, we control the colloidal osmotic pressure. What is controlled in lens is the total osmotic pressure equilibrium with the exterior. The protein concentration difference induced between cortical and cytoplasmic extracts by constant colloidal osmotic pressure now needs to be compared to the *observed* concentration gradient.

What we know about the *in vivo* situation is that, according to e.g. Amoore et al. (1959), the average concentration of the cortical extracts of calf lenses is of the order of  $0.30 \text{ g/cm}^3$  and that of the nuclear extracts of the order of  $0.42$  to  $0.50 \text{ g/cm}^3$ . Also, the preliminary measurements of the colloidal osmotic pressure of proteins reported by Reiff (1986) on cortical and nuclear extracts were respectively  $2.5 \cdot 10^5$  and  $5 \cdot 10^5$  dynes/cm<sup>2</sup> (10 and 20 mOsmoles). These values can be translated using Fig. 3 into protein concentrations of respectively  $0.40$  and, if we extrapolate the nuclear data, about  $0.55$  to  $0.60 \text{ g/cm}^3$ . Such values are higher than those reported by Amoore et al. (1959); their difference is, however, similar:  $0.15$  to  $0.20 \text{ g/cm}^3$  which is about three to four times the difference that we observed.

The *in vivo* concentration gradient is therefore steeper than the one that can be created from constant colloidal osmotic pressure, even if we admit that our separation of cortical and nuclear extracts might not have been perfect.

We therefore find it relevant at this stage to remember that the colloidal osmotic pressure values that we have measured or those measured by Reiff (1986) are quite small compared to the total lens osmotic pressure which is of the order of 300 mOsmoles (Cotlier et al. 1968; Duncan and Jacob 1984), most of it coming from the ions or the small molecules. In fact, to account for the *observed* lens protein concentration gradient as well as for Reiff's measurements, it is sufficient to assume that the total osmotic pressure within lens remains constant but that the proteins have to counterbalance a small additional ion or small molecule concentration gradient in the opposite direction. From our measurements, this additional ion gradient

should be of the order of 5 to 7.5 mOsmoles (corresponding to an additional protein concentration difference of 0.10 to 0.15 g/cm<sup>3</sup>).

This is not unreasonable as previous workers, e.g. Amoore et al. (1959), have reported differences of Na<sup>+</sup> concentration of the order of 15 mM, while recent NMR measurements (Garner et al. 1986) also seem to indicate at lower Na<sup>+</sup> concentration in the nucleus than in the cortex. The pump leak mechanism model is also compatible with an ion gradient within the lens provided this gradient does not present sharp discontinuities. Also, the ion activity may vary from cortex to nucleus with the volume available to the ions.

We thus have a hypothesis for the formation and maintenance of a protein concentration gradient within eye lens, that seems consistent with much of the data already available and that could perhaps be better documented in the future with more local measurements of ion concentrations and activities than those presently available. Such a hypothesis is also relevant to other characteristics of normal and cataractous lens and changes associated with aging. Some speculations leading to predictions, such as those developed below, could also be used to further check the validity of the hypothesis.

An expected consequence of the hypothesis is that the protein solution may act as an 'osmotic buffer' to compensate imbalance of osmotic pressure between adjacent fiber cells due to variations of the small solute (electrolyte and/or amino-acid and/or sugar) concentrations. Since a change in relative osmolarity of 1 mOsmole (whatever its origin, e.g. gap junction blocking, metabolic changes) is expected to be compensated by a change in 0.02 g/cm<sup>3</sup> of the protein concentration, minor changes in local small solute concentrations might thus induce non-negligible changes in protein concentration from one fiber cell to the next. Changes in protein concentration mean changes in refractive index, possibly leading to light scattering and opacities (Tardieu and Delaye 1988). This could represent one of the mechanisms involved in the so-called osmotic cataracts.

Finally, the origin of the body water loss with aging, so nicely documented by Reiff (1986), and in particular the evolution with age of the total lens protein concentration, is readily explained by the process proposed in this paper. The amount of lens insoluble material is known to increase as a function of age. Formation of such material is usually associated with aggregate formation (possibly as a consequence of post translational modifications). Since the colloidal osmotic pressure varies as the inverse of the molecular weight, it decreases with protein aggregation. Reiff (1986) indeed noted that protein aggregation, that he associates with water loss, may result in decreased colloidal osmotic pressure. However, he then inferred

that the colloidal osmotic pressure should be lower in cataractous than in normal lens. Our hypothesis leads us to different predictions. Since the protein quantity within a fiber cell is fixed, whenever part of this protein amount aggregates and decreases its contribution to the colloidal osmotic pressure, the concentration of the remaining non-aggregated protein will increase, in order to restore the original colloidal osmotic pressure. Formation of insoluble material as a function of age would therefore naturally lead to increasing protein concentration as a function of age, until the inner fiber cells become so dense and tightly packed and their protein content so viscous that osmotic regulation is no longer possible. Testing such predictions should be possible in the future.

*Acknowledgements.* We thank Linda Sperling and Patrice Vachette for critical reading of the manuscript. This work is part of the PhD thesis of F. V. and was pursued within the scope of the European Communities Concerted Action on Ageing and Diseases (EURAGE).

## References

- Amoore JE, Bartley W, van Heyningen R (1959) Distribution of sodium and potassium within cattle lens. *Biochem J* 72: 126–133
- Benedek GG (1971) Theory of transparency of the eye. *Appl Opt* 10:459–473
- Bindels JG (1982) Structural studies on soluble lens proteins related to aging. PhD Thesis. Nijmegen
- Campbell MCW (1984) Measurement of refractive index in an intact crystalline lens. *Vision Res* 24:409–415
- Clark JI, Delaye M, Hammer P, Menge L (1982) Preparation and characterization of native lens cell cytoplasm. *Curr Eye Res* 1:695–704
- Cotlier E, Kwan B, Beaty C (1968) The lens as an osmometer and the effects of medium osmolarity on water transport, <sup>86</sup>Rb efflux and <sup>86</sup>Rb transport by the lens. *Biochim Biophys Acta* 150:705–722
- Delaye M, Tardieu A (1983) Short range order of crystallin protein accounts for eye lens transparency. *Nature (London)* 302:415–417
- Delaye M, Danford-Kaplan ME, Clark JI, Krop B, Gulik-Krzywicki T, Tardieu A (1987) Effect of calcium on the calf lens cytoplasm. *Exp Eye Res* 44:601–616
- Duncan G, Jacob TJC (1984) The lens as a physical system. In: Davson H (ed) *The eye*. Academic Press, London New York, pp 159–206
- Eisenberg H (1976) *Biological macromolecules and polyelectrolytes in solution*. Clarendon Press, Oxford
- Garner WH, Hilal SH, Lee SW, Spector A (1986) Sodium-23 magnetic resonance imaging of the eye and lens. *Proc Natl Acad Sci USA* 83:1901–1905
- Goodenough DA, Dick JSB, Lyons JE (1980) Lens metabolic cooperation: a study of mouse lens transport and permeability visualised with freeze-substitution autoradiography and electron microscopy. *J Cell Biol* 86:576–589
- Guinier A, Fournet G (1955) *Small angle scattering of X-rays*. J Wiley, New York

- Huizinga A, Bot ACC, de Mul FFM, Vrensen GFJM, Greve J (1989) Local variation in absolute water content of human and rabbit eye lenses measured by raman spectroscopy. *Exp Eye Res* 48:487–496
- Kinsey VE, Reddy DVN (1965) Studies of the crystalline lens. XI The relative role of the epithelium and capsule in transport. *Invest Ophthalmol* 4:104–121
- Parsegian VA, Rand RP, Fuller NL, Rau DC (1986) Osmotic stress for the direct measurement of intermolecular forces. *Methods Enzymol* 127:400–416
- Piatigorsky J (1981) Lens differentiation in vertebrates. A review of cellular and molecular features. *Differentiation* 19:134–153
- Pierscionek B, Smith G, Augusteyn RC (1987) The refractive increments of bovine  $\alpha$ -,  $\beta$ -, and  $\gamma$ -crystallins. *Vision Res* 27:1539–1541
- Prouty MS, Schechter AN, Parsegian VA (1985) Chemical potential measurements of deoxyhemoglobin S polymerization: Determination of the phase diagram of an assembling protein. *J Mol Biol* 184:517–528
- Reiff TR (1986) A colloid osmotic model of macromolecular aggregation to explain tissue water loss in aging. *Exp Gerontol* 21:267–276
- Siezen RJ, Fisch MR, Slingsby C, Benedek GB (1985) Opacification of  $\gamma$ -crystallin solutions from calf lens in relation to cold cataract formation. *Proc Natl Acad Sci USA* 82:1701–1705
- Siezen RJ, Wu E, Kaplan ED, Thomson JA, Benedek GB (1988) Rat lens  $\gamma$ -crystallins: characterization of the six gene products and their spatial and temporal distribution resulting from differential synthesis. *J Mol Biol* 199:475–490
- Slingsby C (1985) Structural variation in lens crystallins. *TIBS* 10:281–284
- Tardieu A, Delaye M (1988) Eye lens proteins and transparency: from light transmission theory to solution X-ray structural analysis. *Annu Rev Biophys Biophys Chem* 17:47–70
- Thomson JA, Schurtenberger P, Thurston GM, Benedek GB (1987) Binary liquid phase separation and critical phenomena in a protein/water solution. *Proc Natl Acad Sci USA* 84:7079–7083
- Trokel SL (1962) The physical basis for transparency of the crystalline lens. *Invest Ophthalmol* 1:493–501
- Vérétout F, Delaye M, Tardieu A (1989) The molecular basis of eye lens transparency: osmotic pressure and X-ray analysis of  $\alpha$ -crystallin solutions. *J Mol Biol* 205:713–728
- Wistow G, Turnell B, Summers L, Slingsby C, Moss D, Miller L, Lindley P, Blundell T (1983) X-ray analysis of the eye lens protein  $\gamma$  II-crystallin at 1.9 Å resolution. *J Mol Biol* 170:175–202